Reduction of V-pit and threading dislocation density in InGaN/GaN heterostructures grown on cracked AlGaN templates

2008 J. Phys.: Condens. Matter 20 095210

(http://iopscience.iop.org/0953-8984/20/9/095210)

J. Phys.: Condens. Matter **20** (2008) 095210 (6pp) doi:10.1088/0953-8984/20/9/095210

Reduction of V-pit and threading dislocation density in InGaN/GaN heterostructures grown on cracked AlGaN templates

C B Soh[1,3], S Y Chow[1], S Tripathy[1] and S J Chua[1,2,3]

[1] Institute of Materials Research and Engineering, A*STAR (Agency for Science, Technology and Research), 3 Research Link, s(117602), Singapore
[2] Department of Electrical and Computer Engineering, National University of Singapore, Singapore

E-mail: cb-soh@imre.a-star.edu.sg and elecsj@nus.edu.sg

Received 21 December 2007, in final form 22 January 2008
Published 8 February 2008
Online at stacks.iop.org/JPhysCM/20/095210

Abstract
The high density of threading dislocations, often leading to the formation of inverted hexagonal pits in InGaN/GaN heterostructures on sapphire substrates, lowers the radiative efficiency of light emitting devices. In this study, a cracked AlGaN template has been implemented as a strain-relaxed layer for subsequent growth of InGaN/GaN heterostructures. The detailed electron microscopy and surface topographic analyses show that such a template has led to a reduction of threading dislocation density especially for screw dislocations and V-pits in the overgrown InGaN/GaN layers. The relaxed regrowth of such heterostructures also leads to an improved crystalline quality and a higher In incorporation in InGaN. The improvement in the optical and structural quality of these InGaN/GaN layers is investigated by means of photoluminescence spectroscopy and transmission electron microscopy.

(Some figures in this article are in colour only in the electronic version)

1. Introduction

InGaN/GaN heterostructures are widely used as active layers in blue–green light emitting diodes and lasers. However, the lack of suitable lattice matched substrates for GaN growth results in a high density of threading dislocations in epilayers [1]. Formation of these defects in GaN-based layers usually degrades the device performance. In InGaN/GaN heterostructures and multi-quantum wells, inverted hexagonal pits [2, 3] are usually formed and initiated at threading dislocation (TD) sites. These TDs extend along the *c*-axis growth direction in the InGaN layer and terminate as V-pits. Special growth techniques have been used to reduce the density of TDs—such as by epitaxial lateral overgrowth (ELO) [4], Si-delta doping [5] and porous GaN templates [6]. Akasaka *et al* have reported the use of thin $Si_xAl_{1-x}N$ interlayers to reduce TDs in AlGaN grown on SiC substrates [7]. Furthermore, the lattice mismatch between the InGaN and GaN layers results in a composition pulling effect whereby indium atoms are more easily incorporated when there is a strain relaxation in the InGaN epilayer. The In composition and the extent of strain relaxation in the InGaN film progressively increase with the film thickness. It is well known that this anomalous composition pulling affects the emission spectra of quantum wells and their luminescence efficiency [8]. The densities of TDs and V-pits show a drastic increase on the surface when a higher In composition is used for epitaxy of InGaN/GaN heterostructures. To lower the surface pit density and to improve the luminescence properties of InGaN, it is desirable to use strain-relaxed GaN templates. The implementation of cracked GaN template for the regrowth of GaN has been reported [9] and it was found that the growth of such continuous GaN layers on top of the cracked templates reduces the screw dislocation density in the GaN layer by an order

[3] Authors to whom any correspondence should be addressed.

of magnitude. Raghavan *et al* has also reported on the microstructural changes in the surface morphology of GaN epilayers grown on increasing thicknesses of graded AlGaN buffer on Si(111) which he attributed to the reduction in the tensile stress of the subsequent GaN layer [10]. In this work, we report on the use of a strain-relaxed cracked AlGaN template for subsequent regrowth of GaN to minimize density of TDs as well as to reduce the density of V-pits on the subsequent InGaN surface. The growth method could improve the crystalline quality of high In composition InGaN layers on GaN/sapphire templates.

2. Experimental details

The five GaN samples used in this study were grown by metal–organic chemical vapor deposition (MOCVD) at 1020 °C using trimethylgallium (TMG) flow, trimethylindium (TMI) and trimethylaluminum (TMA) as the source gas. A 25 nm thick LT-GaN buffer layer is first grown at 525 °C on sapphire substrate. The temperature was then raised to 1020 °C for the growth of a 1.8 μm thick u-GaN layer. For sample B, C, D and E, a 200 nm thick cracked $Al_wGa_{1-w}N$ ($0.35 < w < 0.43$) template was grown on the 1.8 μm thick u-GaN using trimethylaluminum (TMA) precursor at 1030 °C and a pressure at 60 Torr but for sample A, no $Al_wGa_{1-w}N$ layer was deposited. Such a high Al composition AlGaN layer induces crack formation in the AlGaN template due to mismatch with the underlying GaN [10, 11]. Tripathy *et al* have derived the strain cartography in GaN and AlGaN/GaN superlattices, which shows that the cracking leads to strain relaxation [11]. Regrowth of undoped and Si-doped GaN ($n_s \sim 5 \times 10^{17}$ cm^{-3}) is subsequently carried out on this AlGaN template for sample B, C, D and E with thicknesses of 0.5 μm, 1.0 μm, 1.5 μm and 2.0 μm respectively. The overgrowth process across the cracks leads to a relaxed uniformly flattened region for further growth of the top 180–200 nm $In_xGa_{1-x}N$ ($0.18 < x < 0.20$) layer using trimethylindium (TMI) and trimethylgallium (TMG) at a temperature of 760 °C and a pressure of 100 Torr. For sample A, regrowth of a 1.0 μm/1.0 μm thick u-GaN/Si-doped GaN was carried out before further growth of $In_xGa_{1-x}N$ ($0.18 < x < 0.20$) layer under the same conditions as for the rest of the samples.

The microstructural investigation of these heterostructures was carried out with a Philips CM300 transmission electron microscope. The cross-sectional TEM samples were analyzed to study the behavior of threading dislocations. The surface topography of these overgrown InGaN layers is studied by atomic force microscopy (AFM). The root mean square (rms) surface roughness and surface pit density are used as the measure of surface smoothness in InGaN/GaN heterostructures. Raman measurements of the templates are also carried out to evaluate the crystalline properties. The micro-Raman system uses a 514.5 nm excitation line of an Ar^+ laser, where the scattered light was dispersed through a JY-64000 triple monochromatic system attached to a liquid nitrogen cooled CCD detector.

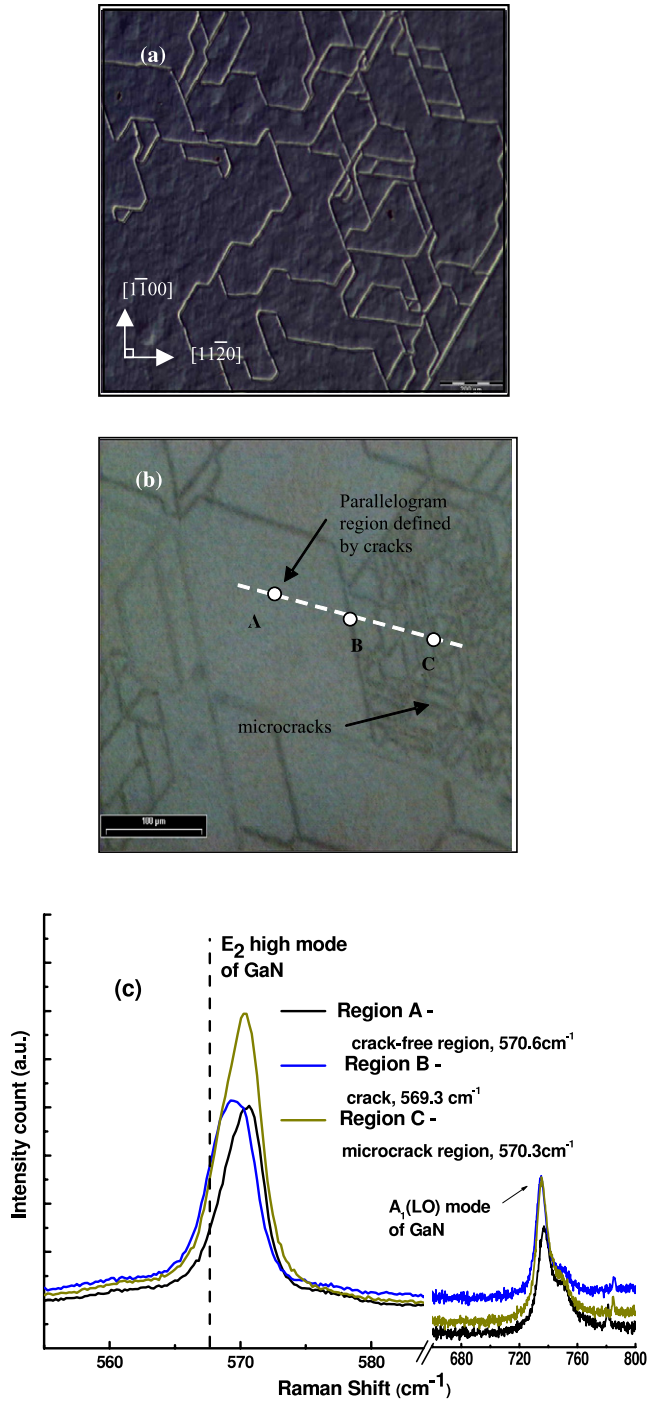

Figure 1. (a) Optical microscopic image of the cracked $Al_{0.43}Ga_{0.57}N$ template. (b) Optical microscope image of a AlGaN/GaN template with a 500 nm thick GaN cap layer. (c) Raman spectra of GaN/AlGaN/GaN heterostructure measured at different locations marked as A, B and C, and indicated in (b). The dashed line marks the E_2 phonon peak of strain-free GaN.

3. Results and discussion

3.1. GaN regrowth on the cracked AlGaN templates

Figure 1(a) shows a typical optical microscopy image of the surface of cracked $Al_{0.43}Ga_{0.57}N$/GaN template on sapphire substrate. This image shows that cracks appear throughout

the surface of AlGaN. The most frequent and recognizable pattern of the cracks followed the hexagonal orientation of the wurtzite lattice. The Al content in the layer was estimated to be about 43% from x-ray diffraction analysis and the thickness of the cracked template determined from SIMS depth profiling is found to be approximately 200 nm. The separation between crack lines ranges from 50 to 250 μm. On the basis of figure 1(a), the propagations of the cracks are mainly in the $[11\bar{2}0]$, $[2\bar{1}\bar{1}0]$ and $[1\bar{2}10]$ directions [12]. For growth of AlGaN on GaN, the strain distribution is normally homogeneous over the whole surface of the sample. There is, however, a certain direction of propagation of these crack lines as growth of GaN layer proceeds from coalescence of hexagonal shaped islands. Cracks on the AlGaN layers are generated mainly along the grain boundaries of the underlying GaN (which is the coalescence plane of its nucleation islands). This accounts for the propagation of cracks with growth of a mismatch thick layer of high composition AlGaN (with high composition, $0.35 < w < 0.43$). The formation of microcracks helps to relieve the strain arising from the film–substrate lattice mismatch while cooling down from the growth temperature of above 1000 °C. Similar patterns of microcracks have been observed in previous study of thick (>13 μm) GaN on sapphire and heavily Si-doped GaN layers [13, 14]. These cracked $Al_{0.43}Ga_{0.57}N$/GaN templates are then used for the overgrowth of Si-doped and undoped GaN interlayers.

In order to determine the extent of strain relaxation in the material, micro-Raman measurement was carried out on the 0.5 μm thick GaN epilayer (sample B) overgrown on AlGaN template. As shown in figure 1(b), location A represents the crack-free region, B represents the region near the cracks while location C is the microcrack region. Figure 1(c) shows the Raman spectra recorded from these locations. The Raman active E_2 optical phonon modes of GaN in different regions show a clear peak shift. For GaN grown on sapphire substrate, the layer is usually under biaxial compressive stress, which accounts for the hardening of the E_2 mode. This Raman peak from the overgrown GaN is observed to be higher than 567.5 cm^{-1} as this is standard from the fully relaxed free-standing GaN substrate of thickness 400 μm. We have observed that there is a substantial reduction in the compressive stress at the cracks (position B) but a less significant reduction of stress in the microcrack region (position C) as evident from the redshift of the E_2 mode from 570.6 cm^{-1} in the crack-free region (position A) as compared to 569.3 cm^{-1} and 570.3 cm^{-1} at positions B and C. The redshift of 1.3 cm^{-1} for spectra, from position C to A, corresponds to stress relaxation in GaN layers of $\sigma = 0.31 \pm 0.05$ GPa, using the equation $\Delta E_2(TO) = K\sigma$ where $K = 4.2$ cm^{-1} GPa^{-1}. Hence, effective reduction of compressive stress occurs for the cracks but not the microcracks which are more likely a surface cracking phenomenon.

The stress distribution in the AlGaN template with a high Al content is dominated by biaxial tensile stress, which leads to cracking. However, overgrown GaN on AlGaN is showing a relaxation of compressive stress, which will be beneficial for the regrowth of InGaN with high indium content. The stress analysis using the three-dimensional finite element method [15, 16] describes how full relaxation can be observed close to the crack region. This explained the substantial stress relaxation close to the cracks observed from the micro-Raman scan. The high density of microcracks is, however, not as effective in relaxation of strain. The effectiveness of the cracks in reduction of threading dislocations will be further analyzed using TEM.

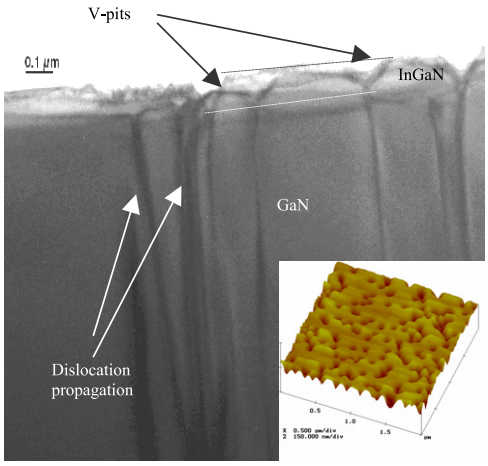

Figure 2. The dark field TEM image taken along $\mathbf{g} = [0002]$ and zone axis $[2\bar{1}\bar{1}0]$ for InGaN/GaN structure, showing a high density of threading dislocation, terminating at the vertex with screw and mixed components. The inset shows the AFM surface topography.

3.2. Regrowth of InGaN/GaN heterostructures

Figure 2 shows the dark field TEM image along $\mathbf{g} = 0002$ and zone axis $[2\bar{1}\bar{1}0]$ for a typical InGaN/GaN heterostructure directly grown on GaN/sapphire templates without strain-relaxed templates. The threading dislocations, which are mainly of mixed and screw type, are linked to the vertex of the V-pits. It was also observed that some of the dislocations are terminated before reaching the epilayer, but most of the threading dislocations are terminated at the vertices of V-pits at the InGaN epilayer. Gliding of threading dislocations along different planar directions leads to dislocation branching and formation of additional surface pits. The V-pit formation serves as a mechanism for relaxation of these terminated dislocations. The inset gives the three-dimensional atomic force microscopy image over a 2.0 μm × 2.0 μm scan region, which clearly shows a high density of V-pits in the InGaN film of 8.5 × 10^8 cm^{-2}.

As discussed earlier, the cracked AlGaN template serves as an effective layer for strain relaxation. Thus, we have attempted to grow the InGaN/GaN heterostructure with the use of an AlGaN/GaN template for reduction of surface pits. Figure 3(a) shows the cross-sectional SEM image of the InGaN/GaN/AlGaN heterostructure with undoped GaN and Si-doped GaN interlayers, each of thickness 1.0 μm. The thickness of these interlayers is also determined from the SIMS depth profiling. It appears that pit formation has been minimized with the implementation of the cracked AlGaN template, where minimal surface pit density is observed

from both top-view SEM and AFM micrographs. With the insertion of such a cracked $Al_{0.4}Ga_{0.6}N$ layer, most of the dislocation propagation is hindered at the AlGaN layer through termination and looping toward the underlying layer. This reduces the overall dislocation density in the subsequent top InGaN/GaN layers.

To determine the quality of the GaN and the behavior of the threading dislocations with insertion of the cracked AlGaN layer, cross-sectional TEM analysis is carried out and two beam conditions are utilized. The weak beam dark field TEM images are taken with $g = [0002]$ and $g = [01\bar{1}0]$, which enables us to identify the screw dislocations (S) with $\boldsymbol{b} = [0002]$ in figure 3(b) and the edge dislocations (E) with $\boldsymbol{b} = (1/3)[11\bar{2}0]$ in figure 3(c) individually. Mixed dislocations (M) with $\boldsymbol{b} = (1/3)[11\bar{2}3]$ can be observed in both the weak beam images, according to the invisibility criteria. By comparison of the images in the different glide planes, it appears that the densities of screw dislocations have been substantially reduced while there is not as much reduction for the edge and mixed dislocations. Such a growth approach may be suitable for the fabrication of InGaN/GaN photonic devices with a high In content.

The purpose of the growth of the undoped GaN and Si-doped GaN interlayers is to provide a kind of lateral overgrowth so that no crack propagation takes place in the top layers. A morphology study was conducted for the set of samples with varying interlayer thickness of undoped and Si-doped GaN (with $n_s \sim 5 \times 10^{17}$ cm^{-3}) to determine whether the cracks in the AlGaN layer have been effectively filled up and the V-pit density in the top layer is reduced. The four samples labeled as B, C, D and E represent the use of varying thickness of GaN interlayers. The measured rms surface roughness of the samples is shown in table 1. When the thickness of the Si-doped GaN interlayer is about 0.5 μm (with no u-GaN layer), the microcracks propagate through the GaN interlayer to reach the InGaN epilayer as there is no effective crack filling by overgrowth. As shown in the AFM micrograph of figure 4(a), the V-pits appear to be associated with the microcracks as they are linked to the network of the cracks. These microcracks serve as strain relief regions; hence dislocations tend to release strain energy through pit formation close to the cracked region. This also explained the segregation of the pits close to the vicinity of the microcracks. As the thickness of the interlayer increases to 0.5 μm Si-doped GaN/0.5 μm undoped GaN (topography in figure 4(b)), the cracks become more effectively filled. However, growth of the InGaN epilayer shows stripe-like surface undulations layers which are defined by the area enclosed by microcracks. In this case, the pits appeared to be filled by the top InGaN layer as only shallow indentation is observed and surface roughness is reduced from 3.3 to 1.5 nm. Further increase in the thickness of the GaN interlayers causes the complete lateral overgrowth of the InGaN layer and the surface roughness to be further reduced to 1.3 nm. The V-pit density on the surface of InGaN has been substantially reduced as shown in the AFM image (figure 4(d)). On the basis of the results from this set of samples, we can conclude that the cracked AlGaN layer serves as an effective template for the reduction of V-pit density in the InGaN epilayer. The overall surface roughness is slightly higher due to the thicker InGaN growth as compared to the case for conventional InGaN/GaN quantum wells.

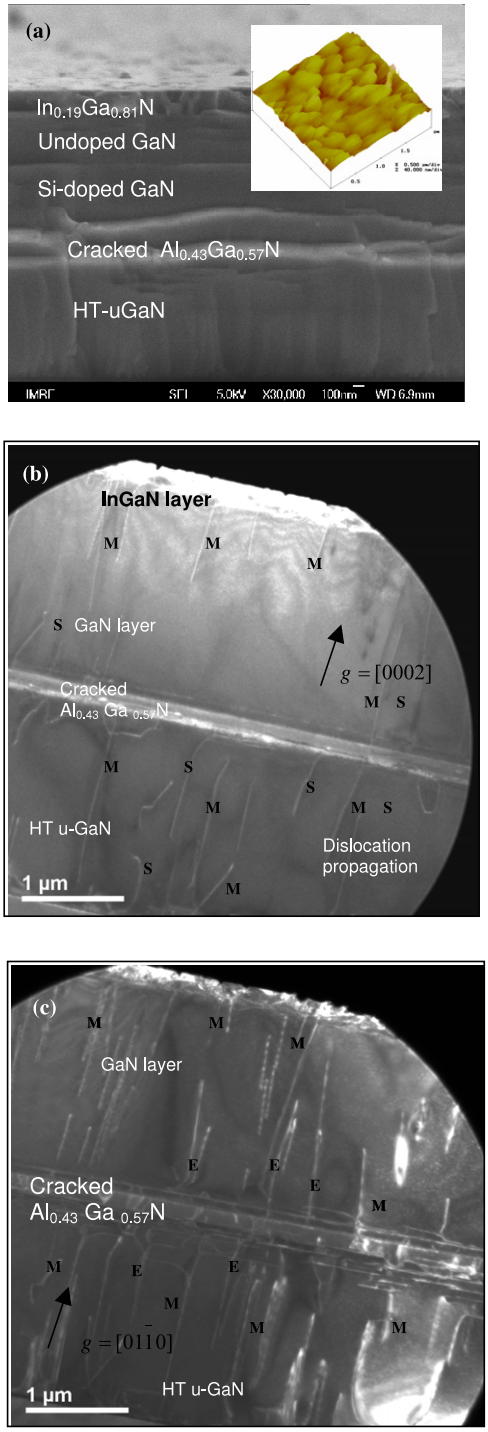

Figure 3. (a) The cross-sectional SEM image of sample E with an overgrown InGaN/GaN epitaxial layer with a strain-relaxed cracked AlGaN template. The inset shows the AFM topography of this structure with the absence of V-pits. Cross-sectional weak beam dark field TEM images of sample E taken with (b) $g = [0002]$ and (c) $g = [0\bar{1}10]$. The images show (b) dislocations with screw components, particularly $\boldsymbol{b} = [0002]$ and $\boldsymbol{b} = (1/3)[11\bar{2}3]$ in GaN. (c) Dislocations with edge components, particularly $\boldsymbol{b} = (1/3)[11\bar{2}0]$ and $\boldsymbol{b} = (1/3)[11\bar{2}3]$ in GaN.

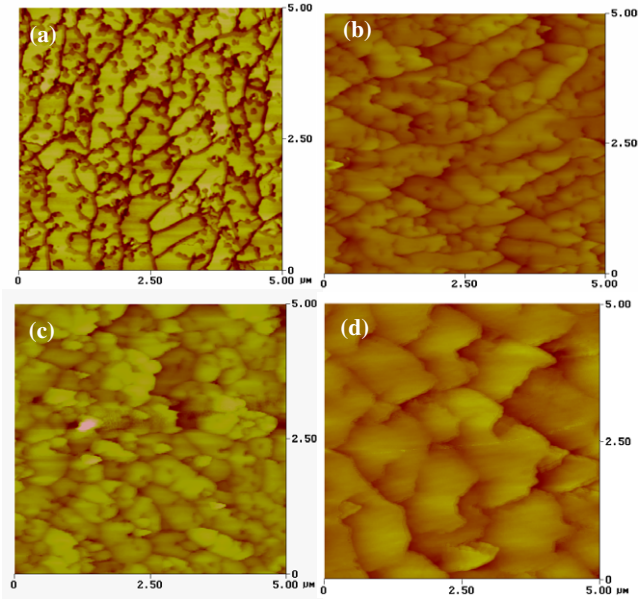

Figure 4. AFM images of InGaN epilayers with different thicknesses of u-GaN/n-GaN interlayers; (a) only 0.5 μm n-GaN, sample B; (b) 0.5 μm u-GaN/0.5 μm n-GaN, sample C; (c) 0.5 μm u-GaN/1.0 μm n-GaN, sample D; and (d) 1.0 μm u-GaN/1.0 μm n-GaN, sample E. Structure (d) shows an overall reduction of dislocation density and surface pit density by an order of magnitude.

Table 1. Samples with varying thickness of u-GaN/n-GaN interlayers and the corresponding overgrown InGaN surface roughness.

Sample	Thickness of u-GaN (μm)	Thickness of n-GaN (μm)	Average rms roughness (nm)
B	0	0.5	3.3
C	0.5	0.5	1.5
D	0.5	1.0	1.3
E	1.0	1.0	1.3

3.3. Effect of interlayer thickness on PL emission

Figure 5 shows the microphotoluminescence (PL) spectra of such InGaN/GaN heterostructures grown on top of GaN interlayers with varying thickness. The 325 nm He–Cd laser beam was focused to a 2.0 μm spot and the excitation power was kept below 200 μW during PL measurements. The band-edge emission peak from InGaN is observed near 486 nm, which shows a substantial redshift from the InGaN/GaN heterostructure on a conventional GaN/sapphire template of similar In composition. Sample A with the InGaN/GaN structure simultaneously grown on sapphire without the AlGaN template shows the PL peak at 452 nm. This observation suggests a higher incorporation of indium in InGaN epilayers with the use of the AlGaN template. Besides the main dominant peak, the spectra also show a broad yellow luminescence (YL) band centered around 550 nm. With only about 0.5 μm Si-doped GaN interlayer, the PL spectrum from the heterostructure gives a higher YL emission intensity. This is an indication of the high defect density

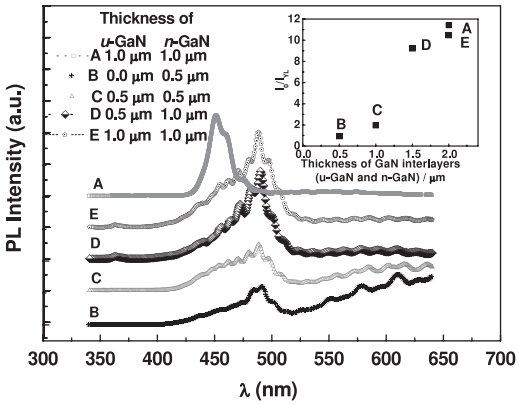

Figure 5. The room temperature microphotoluminescence spectra recorded from the InGaN/GaN/AlGaN heterostructure with varying thickness of GaN interlayers grown. The inset shows the plot of the PL intensity ratio I_0/I_{YL} versus the samples with varying thickness of the GaN interlayers.

in the InGaN epitaxial film due to the presence of surface defects. The highly cracked region (as shown by the AFM image in figure 4(a)) serves as non-radiative recombination trapping sites as impurities tend to segregate to regions with minimal strain. This competes with the band-edge emission of the InGaN epilayer and led to a higher YL intensity I_{YL}, as impurities formed complexes such as O_N which can be decorated along pits and dislocation lines in the close vicinity of cracks. With further increase in the thickness of the GaN interlayers, the band-edge emission becomes more pronounced while the yellow band is suppressed.

When GaN film starts to grow on the cracked AlGaN template, a substantial reduction of dislocations is observed at the [0002] plane, suggesting a greater extent of lateral overgrowth to nucleate the GaN layer on the AlGaN template. Most of the screw dislocations with $\boldsymbol{b} = [0002]$ have been terminated or bent at the cracked AlGaN template. The strain released GaN overgrown on the cracked AlGaN layer leads to a more uniform 2D growth of the GaN/InGaN epilayer. This reduces the V-pit formation as the V-pits originate from threading dislocations. The defect/impurity decorations at the cracks are substantially suppressed, as growth at high temperature (>1000 °C) for GaN interlayer enhances the mobility of the adatoms to give a 2D lateral overgrowth. Structural defects and the dislocations are terminated within the GaN interlayer if it is of sufficient thickness (∼1.5 μm as shown in figure 4(c)). The Si dopants in the n-GaN layer further screen the carriers from the effect of scattering by dislocations [9], which enables a high optical quality InGaN/GaN heterostructure via subsequent overgrowth. This contributed to the stronger band-edge PL emission from the InGaN peak (I_0) and a suppressed YL emission, I_{YL}. The inset in figure 5 shows the ratio I_0/I_{YL} for the case of InGaN layers with varying thicknesses of interlayers. The PL analysis shows an improved I_0/I_{YL} ratio for InGaN/GaN heterostructures grown on cracked AlGaN templates with about 1.5 and 2.0 μm thick GaN interlayers. The conventional InGaN/GaN heterostructure, sample A, has an I_0/I_{YL} ratio comparable to sample E's, illustrating that defect/impurity decoration has

been effectively suppressed in the cracked AlGaN layer with growth of a 2.0 μm thick GaN interlayer.

4. Conclusions

In summary, we have investigated microstructural properties of InGaN/GaN heterostructures grown on strain-relaxed cracked AlGaN/GaN/sapphire templates. Introduction of this AlGaN template and subsequent regrowth of GaN/InGaN heterostructures led to a reduction of the densities of TDs and V-pits. To minimize the dislocation density in such InGaN/GaN top layers, an effective control of the interlayer thickness, MOCVD conditions such as the gas flow, pressure and temperature is essential. AFM study shows that we can achieve a substantial reduction in pit density by more than an order of magnitude. This growth technique may be suitable for the overgrowth of high optical quality and higher In content epilayers for photonic device use.

References

[1] Narayanan V, Lorenz K, Kim W and Mahajan S 2001 *Appl. Phys. Lett.* **78** 1544
[2] Srinivasan S, Geng L, Liu R, Ponce F A, Narukawa Y and Tanaka S 2003 *Appl. Phys. Lett.* **83** 5187
[3] Hiramatsu K 2001 *J. Phys.: Condens. Matter* **13** 6961
[4] Beaumont B, Vénneguès P and Gilbart P 2001 *Phys. Status Solidi* b **227** 1
[5] Wang L S, Zang K Y, Tripathy S and Chua S J 2004 *Appl. Phys. Lett.* **85** 5881
[6] Soh C B, Hartono H, Chow S Y, Chua S J and Fitzgerald E A 2006 *Appl. Phys. Lett.* **90** 053112
[7] Akasaka T, Nishida T, Taniyasu Y, Kasu M, Makimoto T and Kobayashi N 2003 *Appl. Phys. Lett.* **83** 4140
[8] Soh C B, Chua S J, Liu W, Lai M Y and Tripathy S 2005 *Solid. State. Commun.* **136** 421
[9] Soh C B, Chua S J, Lim H F, Chi D Z, Liu W and Tripathy S 2004 *J. Phys.: Condens. Matter* **16** 6305
[10] Raghavan S and Redwing J 2005 *J. Appl. Phys.* **98** 023515
[11] Tripathy S, Chua S J and Miao Z L 2002 *J. Appl. Phys.* **92** 3503
[12] Pernot J, Bustarret E, Rudzinski M, Hageman P R and Larsen P K 2007 *J. Appl. Phys.* **101** 033536
[13] Bernard G 1998 *Group III Nitride Semiconductor Compounds: Phys and Appl* (Oxford: Clarendon) chapter 3 (MOPVE Growth of Nitrides)
[14] Itoh N, Rhee J C, Kawabata T and Koike S 1985 *J. Appl. Phys.* **58** 1828
[15] Rudloff D *et al* 2003 *Appl. Phys. Lett.* **82** 367
[16] Einfeldt S, Dießelberg M, Heinke H, Hommel D, Rudloff D, Christen J and Davis R F 2002 *J. Appl. Phys.* **92** 118